Barker, P.F., Camerlenghi, A., Acton, G.D., and Ramsay, A.T.S. (Eds.)
Proceedings of the Ocean Drilling Program, Scientific Results Volume 178

30. Defining Petrophysical Units of the Palmer Deep Sites from Leg 178[1]

Kate L. Hatfield,[2] Andrew J. Evans,[3] and Peter K. Harvey[4]

ABSTRACT

Palmer Deep, on the inner continental shelf southwest of Anvers Island off the Antarctic Peninsula, is a glacially overdeepened basin consisting of three subbasins. Two sites, 1098 and 1099, were drilled in the Palmer Deep area.

A high-resolution porosity curve has been calculated from density data and subsequently plotted against the shipboard lithologic logs. These new data correspond accurately to the lithologic logs, magnetic susceptibility, and gamma ray attenuation (GRA) density data and offer information on the heterogeneity of the sediments.

Petrophysical groups have been generated to investigate interrelationships between different physical attributes. To develop these petrophysical groups, crossplots of the available physical properties data were performed. The results for the GRA density and magnetic susceptibility crossplots demonstrate distinct clusters. Plotting the magnetic susceptibility and GRA density data logs (divided into these new petrophysical groups) against lithology provided information to subdivide the lithologic unit(s) into a series of petrophysical units.

INTRODUCTION

Sites 1098 and 1099 are located in Palmer Deep on the inner continental shelf southwest of Anvers Island, off the Antarctic Peninsula (Fig. F1). Drilling in Palmer Deep (Sites 1098 and 1099) was aimed at reconstructing the most recent glacial history of the Antarctic Peninsula, through the recovery of a Holocene, and possibly latest Pleistocene, paleoproductivity record representative of regional climate at a decadal

F1. Location map of Palmer Deep, p. 9.

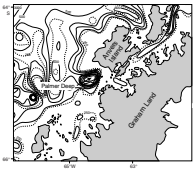

[1]Hatfield, K.L., Evans, A.J., and Harvey, P.K., 2002. Defining petrophysical units of the Palmer Deep sites from Leg 178. *In* Barker, P.F., Camerlenghi, A., Acton, G.D., and Ramsay, A.T.S. (Eds.), *Proc. ODP, Sci. Results,* 178, 1–17 [Online]. Available from World Wide Web: <http://www-odp.tamu.edu/publications/178_SR/VOLUME/CHAPTERS/SR178_30.PDF>. [Cited YYYY-MM-DD]
[2]Amerada Hess Ltd., 33 Grosvenor Place, London, SW1X 7HY, United Kingdom. **kate.hatfield@hess.com**
[3]School of Geography, Leeds University, Leeds, LS2 9JT, United Kingdom.
[4]Geology Department, Leicester University, Leicester, LE1 7RH, United Kingdom.

Initial receipt: 30 July 1999
Acceptance: 17 October 2001
Web publication: 21 February 2002
Ms 178SR-201

and millennial scale. Palmer Deep is a glacially overdeepened basin consisting of three subbasins aligned in an approximately southwest-northeast direction (Fig. F2). These basins contain an ultra high resolution Holocene record of Antarctic Peninsula climate (Leventer et al., 1996).

Site 1099 is located in Basin III, which contains three major acoustic units; the uppermost (~0–70 mbsf; the midbasin reflector) shows similar character to the fill of Basin I (Barker, Camerlenghi, Acton, et al., 1999). Site 1098 was drilled at the southwestern end of Basin I, where sediment fill is draped, contrasting with the overall ponded geometry of the rest of the basin. Each site was assigned a single lithostratigraphic unit (Unit I), and Site 1098 was subsequently subdivided into Subunits IA and IB. Sedimentation in Basin III was recognized by the shipboard party (Barker, Camerlenghi, Acton, et al., 1999) as more affected by mass flow than in Basin I. Additional stratigraphic data derived from piston cores, including radiocarbon dating in Basin III (Kirby et al., in press), suggest that the base of Unit I, as well as the deeper units, may predate the most recent glaciation on the shelf (the last glacial maximum). The seismic units below the midbasin reflectors were therefore considered to be older than the basin-fill unit of Basin I. The basins have some similar depositional environments, but they are also affected by local events and are therefore not directly comparable.

SITES 1098 AND 1099

Three holes (1098A, 1098B, and 1098C) were drilled at Site 1098, and the data from all three were highly comparable. Hole 1098C was drilled to a depth of 46.7 meters below seafloor (mbsf) and was chosen for this study, as it had additional discrete samples taken for physical properties measurements. Two holes were drilled at Site 1099, Hole 1099A (0–62.3 mbsf) and Hole 1099B (60.0–107.5 mbsf). These holes were geographically close enough to enable them to be joined at the chosen depth of 60 mbsf.

Sediments recovered at Sites 1098 and 1099 consist of alternating massive muddy diatom oozes, laminated mud-bearing diatom oozes, and diatom-bearing silty clays and clayey silts with a generally low sand content. In Hole 1098C, ice-rafted pebbles increase in number downhole and at the base of the hole a further increase in coarse clastic material and pebbles is observed. Figures F3 and F4 give the lithostratigraphy of Sites 1098 and 1099, respectively; the lithologic key is given in Figure F5.

Multisensor track (MST) measurements were collected at both Sites 1098 and 1099 (Barker, Camerlenghi, Acton, et al., 1999). These included magnetic susceptibility (MGS) taken every 2 cm (averaged over 2 s), gamma ray attenuation (GRA) density, again taken every 2 cm (averaged over 2 s), and natural gamma radiation counts taken every 15 cm (averaged over 15 s). In addition, physical properties were measured on discrete samples (5–10 cm^3), taken on approximately two sections per 10 m of core. On these samples, a saturated mass, dry mass, and dry volume were measured, from which porosity and bulk density were calculated (Blum, 1997).

F2. Locations of Sites 1098 and 1099, p. 10.

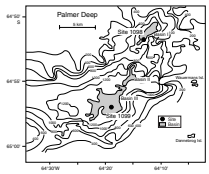

F3. Lithology, magnetic susceptibility, and GRA density, Hole 1098C, p. 11.

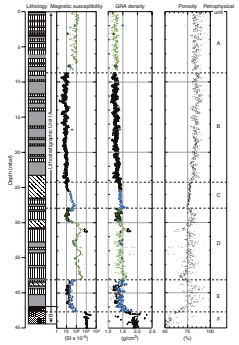

F4. Lithology, magnetic susceptibility, and GRA density, Holes 1099A and 1099B, p. 12.

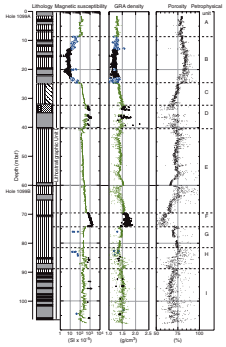

F5. Lithologic and petrophysical group key, p. 13.

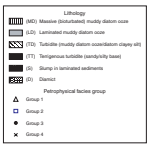

Predicting Porosity Using GRA Density

The derived porosity and bulk density values made on discrete samples taken from the core have been crossplotted (Fig. F6A) and give a significant relationship (r = 0.998 for both sites); 1 known erroneous point was removed out of 48. The values of porosity and bulk density are generated from the same set of three measurements made on the discrete samples and are related by definition; therefore, the relationship between the variables is only quasi-independent.

Evaluation of the bulk density was achieved by crossplotting values against the GRA density (Fig. F6B). Two extra data points were removed from Figure F6B, which gave a significant relationship for both Hole 1098C and Site 1099 (r = 0.967 and 0.889, respectively). Site 1099 tends to give consistently lower GRA density values than the bulk density. Given the strong correlation between bulk density and GRA density, a high-frequency bulk density data set was generated, and from the significant relationship between bulk density and porosity (Fig. F6A), a high-frequency porosity data set was calculated from the newly generated bulk density.

F6. Bulk density vs. porosity and GRA density, p. 14.

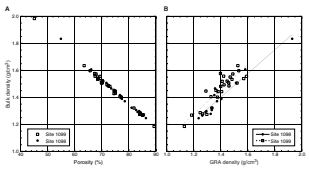

Defining Petrophysical Groups

Petrophysical units have been defined to confirm and constrain the lithologic sequence and also to determine whether there is additional detail present that is not captured within the lithologic logs (Figs. F3, F4).

The groups for Hole 1098C (Fig. F7A) are split as follows: Group 1 has MGS values approximately <20; Group 2 has values with a MGS between 20 and 100 and GRA values approximately >1.35 g/cm^3. Group 3 MGS values fall between 10 and 600 with varying GRA values. Group 4 is characterized by MGS values >600. The groups for Site 1099 (Fig. F7B) are split in a similar, but not identical, manner to those in Hole 1098C. Group 1 has MGS values between 1 and 13; Group 2, between 13 and 60; Group 3, between 60 and 600; and Group 4, all points with MGS values >600.

F7. GRA density vs. magnetic susceptibility, p. 15.

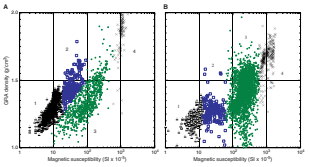

Variation in Petrophysical Characteristics with Depth

The extent to which the clustering of data shown in Figure F7 may be attributed to lithologic variation is demonstrated in Figures F3 and F4. These figures show the lithologic log, MGS, GRA density, and porosity curves for both sites. The MGS and GRA density data are split into the four petrophysical groups defined in the previous section. The lithologic and petrophysical key is given in Figure F5.

The physical properties shown in Figures F3 and F4 do not show smooth graduation downhole. Zones can be picked out visually using the dominant petrophysical groups and character changes within the data. Use of these features enables a series of petrophysical units to be defined.

The porosity curve for Figure F3 decreases steadily downhole (0–38 mbsf) from ~85% to 70%, when it then shows an obvious positive step; the GRA density illustrates the opposite. The MGS data is heterogeneous downhole and has been used in many instances to define the petrophysical units. The turbidites at ~25 and 30 mbsf show graded densities, and this is reflected in the MGS, which generally increases with increasing grain size.

Figure F3 shows how the lithologic log for Hole 1098C, in which one lithostratigraphic unit is defined (divided into Subunits IA and IB), can be subdivided into six petrophysical units using the petrophysical Groups 1–4 defined in Figure F7A. The six petrophysical units are labeled A–F (Fig. F3), and their defining features are listed in Table T1.

T1. Defining characteristics for petrophysical units, Site 1098, p. 16.

The petrophysical Units A and B were recorded as the same lithologies (Barker, Camerlenghi, Acton, et al., 1999), but the response of the MGS data illustrates that the sediment in Unit B is different and is possibly derived from a different source material than Unit A. Preliminary investigations of diatom species assemblages recovered from Sites 1098 and 1099 contribute toward explaining environmental variation in the basins.

A 0- to 9-mbsf piston core recovered at the Site 1098 location (Leventer et al., 1996) revealed that laminated sediments (low magnetic susceptibility) and massive, bioturbated sediments (high magnetic susceptibility) were characterized by different diatom assemblages. Comparison between similar lithologies in petrophysical Units A and B show that the variation cannot simply be due to a change in the percentage of different lithologies. There is real intralithologic variation between the two petrophysical units.

The lithologic and petrophysical logs for Holes 1099A and 1099B are shown in Figure F4. The porosity curve for Figure F4 is very heterogeneous with a decrease of 10% from 0 to 110 mbsf, but values vary by 35% in between and the data show a high degree of scatter. The MGS data vary between three orders of magnitude, but the changes are sharp and scatter is limited. The one lithologic unit can be subdivided into nine units using the petrophysical Groups 1–4 defined in Figure F7. The nine units are labeled A–I (Fig. F4), and their defining features are listed in Table T2.

T2. Defining characteristics for petrophysical units, Site 1099, p. 17.

DISCUSSION

Generally, the low variability of the physical properties in the holes can be attributed to biogenic mixing. This effect is particularly noticeable at Site 1099, where the low-variability material between 40 and 87 mbsf is almost completely bioturbated. The porosity in both holes increases in variability toward their bases; this may be a result of gas fracturing on depressurization and warming on deck. However, it may equally be a result of the increase in pebbles >0.5 cm in both holes at these depths, as reported by the shipboard party (Barker, Camerlenghi, Acton, et al., 1999). Hole 1098C has the additional possibility that the porosity variation reflects the increased slumping observed in the beds toward the base of the hole.

Lower absolute levels of porosity below 25 mbsf at both sites are associated with the poorer diatom preservation noted by the shipboard party (Barker, Camerlenghi, Acton, et al., 1999), whereas the high-porosity, diatom-rich, laminated sediments have better preserved diatom chains and spines than the bioturbated units. It is therefore likely that the low density values reflect a semi-interlocked skeleton of biosiliceous material. Little laboratory research has been done in this area, but it would appear possible on the basis of the rapid change in attributes here that consolidation does not take place in such high diatom concentration sediments until the overburden stress reaches the yield strength of the diatom chain links and spines that support the skeleton.

The porosity and consolidation properties of diatom-containing materials were found to be complex and only partly related to overburden stress by Bryant and Rack (1990) and Pittenger et al. (1989). However, neither study dealt with the depth range in question here, examined diatom damage, or looked at such high concentrations of biogenic material; therefore, the question will have to remain open until laboratory studies can be completed. Both the quoted studies note that at greater depths the internal space of the diatoms gives sediments a higher than expected porosity, and this will also be acting here. In addition, the homogeneity of the diatom species and limited size range in the laminated layers will allow a more porous structure to develop in the same manner as a well-sorted mineral skeleton.

Such factors may explain why the MGS and porosity appear to be inversely related in both holes. The high water content resulting from these processes reduces the bulk density and susceptibility (Bryant and Rack, 1990). Bioturbated layers have poorer diatom preservation, and the effect on porosity may be an additional reason for the finding by Leventer et al. (1996) that bioturbated intervals tended to have a high MGS in the upper 6 mbsf of Basin I. It is likely, however, that the MGS and porosity signals are linked in a manner other than simple volume considerations. For example, a high biogenic content will produce a higher porosity; contrary to this, Leventer et al. (1996) observed that it may also produce a geochemical environment suitable for the removal of susceptible minerals. It is likely, therefore, that the relative importance of volume effects will change with time (and hence, depth). Given the nonlinear relation with depth and without a more detailed study of the mineralogy, it is not appropriate to estimate the effect of porosity on MGS through normalization of the latter's record.

Holes 1098C and 1099A both reveal a trough in the MGS signal and a corresponding high in the porosity data between ~8 and 25 mbsf. Leventer et al. (1996) place the highest point of this trough at 2600 corrected radiocarbon years before present (6 mbsf in their core). Shipboard calculations place the low point at ~11,000 yr before present. Higher MGS and lower porosity levels below this lie directly above diamict units (Hole 1098C [43–45 mbsf] and Site 1099 [32–35 mbsf]). Although the return to high values downcore is obliterated in Hole 1099A by a turbidite, the pattern can be estimated from the MGS levels in the turbidite material (25–32 mbsf) and the material directly below the diamict sequence.

It might be suggested that such a coincidence across holes represents further dating-independent evidence that the diamict at the base of Hole 1098C and that at ~32 mbsf in Hole 1099A (the midbasin reflector) (Barker, Camerlenghi, Acton, et al., 1999) are the same unit. However, there are some inconsistencies between the low-MGS periods in the two holes. The porosity levels inversely match the MGS variation at Site 1099; in Hole 1098C, a porosity rise is less clear and the Hole 1098C MGS signal may also be affected by lower terrigenous inputs at these depths, as seen by the shipboard party (Barker, Camerlenghi, Acton, et al., 1999).

Leventer et al. (1996) have suggested that this trough represents a raised biogenic sedimentation rate during this period, based largely on the presence of raised levels of total organic carbon (TOC) in the portion of the trough they recovered. Shipboard analyses suggest the TOC levels for both holes (Barker, Camerlenghi, Acton, et al., 1999) show peak values matching the complete troughs in both holes. A higher biogenic sedimentation rate convincingly explains both the higher bio-

genic component of the sediment and the porosity, which would reflect a more complete biogenic skeleton and lack of sufficient time to undergo normal consolidation. Such an explanation must await further dating and sedimentary analysis for confirmation but may link the two diamicts more convincingly and could push back the start of the climatic optimum, which Leventer et al. (1996) claim is responsible for the sedimentation rate change.

The laminated ooze (35–40 mbsf) immediately below the diamict in Hole 1099A carries a signal continuous with that of the diamict and distinct from surrounding sediment. Shipboard smear slides suggest sand and silt levels increase up through these materials with high variabilities (Barker, Camerlenghi, Acton, et al., 1999), which are well reflected in the physical properties. Such a continuum between the two lithologies may well point to the diamict being deposited through a water column and the lithology being controlled solely by ice proximity. It could be suggested that the two lithologies are partly mixed and the diamict terrestrial. However, as they are associated by petrophysical classification, the argument for glaciomarine/lacustrine deposition can be enhanced by examining the porosity of the materials, which is relatively large for a subglacial diamict even compared with high porosity subglacial material (cf. 40%) (Ronnert and Mickelson, 1992). Thus, the evidence is consistent with Basin III being a subglacial lake during the diamict deposition; however, the porosity of the diamict at the base of Hole 1098C is much more consistent with terrestrial subglacial material, possibly suggesting the ice was grounded in the shallower Basin I.

The turbidites in the sequences appear to be strongly associated with an increase of MGS and a decrease in porosity with depth. This is to be expected, with coarse-grained terrigenous material being concentrated at the sequence base, giving it a higher susceptibility, and the high-energy deposition going some way to destroying any diatomaceous sediment skeleton. However, in petrophysical Unit C of Hole 1098C and Unit F of Hole 1099C, there are turbidites for which the ramping of these attributes does not coincide with the lithologic limits of the turbidite. The turbidites appear to have affected the material below them without affecting their lithologic appearance. An example is in Hole 1098C, where this process includes the preservation of laminated sediments, suggesting that the material below the turbidites is overprinted with the turbiditic signature. This may occur by settling of small amounts of the high-MGS material into the shear liquefied and unconsolidated seabed sediments that are overrun or by compression and/or flow parallel shear. Given the order of magnitude difference in magnetic susceptibility, any small quantity of terrigenous sediment introduced to the diatomaceous material may swamp the original MGS record with little consequence for the particle size range of the material. This effect is most noticeable in Hole 1098C, where the material between 27 and 28 mbsf is overprinted by the turbidite. The material between 28 mbsf and the top of the next turbidite at 29.5 mbsf could reasonably be assumed identical to that in petrophysical Unit B. The mismatch between the turbidite material at 71 mbsf in Holes 1099A and 1099B and the associated events in the MGS and porosity records between 70 and 74 mbsf may be due to a similar process; however, the more homogeneous nature of the material below the lithologic trace of the turbidite in this case makes it impossible to stipulate that this lower material is not a reworked flow.

SUMMARY AND CONCLUSIONS

The physical properties measurements made on both discrete samples (porosity and bulk density) and the MST (magnetic susceptibility and GRA density) for Palmer Deep Sites 1098 and 1099 are described. Three boreholes are studied, Hole 1098C and a single section joined from the geographically close boreholes 1099A and 1099B.

Cross-correlation of bulk density and GRA density has enabled validation of the GRA measurements, from which a high-resolution porosity curve has been derived for both analyzed sections. Four distinct petrophysical groups were observed for each borehole from a simple visual examination of magnetic susceptibility crossplotted with GRA density.

Plotting the variation in petrophysical group, magnetic susceptibility, GRA density, and the derived high-resolution porosity vs. depth for both sites revealed that each borehole could be zoned into a number of distinct petrophysical units based on the dominant petrophysical group(s), along with the magnitude and variance of the other properties. These petrophysical zones provide a much greater subdivision of the sedimentary sequence than was possible from the shipboard core descriptions.

Whereas some of the observed zoned unit boundaries coincide with recognized lithologic boundaries, most do not, and clearly there are boundaries within the sedimentary sequence that are not apparent from a visual description of the core. The petrophysical classifications draw attention to the alteration of magnetic susceptibility levels in the upper 25 m of both sections. The porosity data add to the evidence that this variation may be due to climate-induced changes in biogenic sedimentation rates, as suggested by Leventer et al. (1996), while also adding another mechanism for the susceptibility signal variations. The data also suggest that the diamict at Site 1099 is petrographically graded with water-lain sediments, suggesting that the diamict may also be water lain. This argument is backed up for the diamict at Site 1099 by high porosities, whereas the diamict at the base of Hole 1098C is closer to terrestrially lain diamict porosities. Finally, evidence is given for the overprinting of the physical properties of nonturbidite materials by turbidites, as well as evidence that the turbidites may only rework shallow sediments from near the seabed surface.

The results show, generally, the usefulness of cross-correlation for determining variations in the materials examined that are invisible to the eye, particularly in delimiting units in bioturbated material, using a methodology can be used during the short time periods available during Ocean Drilling Program (ODP) legs.

ACKNOWLEDGMENTS

This research used samples and/or data provided by the Ocean Drilling Program (ODP). ODP is sponsored by the U.S. National Science Foundation (NSF) and participating countries under management of Joint Oceanographic Institutions (JOI), Inc. Funding for this research was provided by an ODP Rapid Response grant.

REFERENCES

Barker, P.F., Camerlenghi, A., Acton, G.D., et al., 1999. *Proc. ODP, Init. Repts.,* 178 [CD-ROM]. Available from: Ocean Drilling Program, Texas A&M University, College Station, TX 77845-9547, U.S.A.

Blum, P., 1997. Physical properties handbook: a guide to the shipboard measurement of physical properties of deep-sea cores. *ODP Tech. Note,* 26 [Online]. Available from World Wide Web: <http://www-odp.tamu.edu/publications/tnotes/tn26/INDEX.HTM>.

Bryant, W.R., and Rack, F.R., 1990. Consolidation characteristics of Weddell Sea sediments: results of ODP Leg 113. *In* Barker, P.F., Kennett, J.P., et al., *Proc. ODP, Sci. Results,* 113: College Station, TX (Ocean Drilling Program), 211–223.

Kirby, M.E., Domack, E.W., Ishman, S.E., and McClennen, C.E., in press. Magnetic stratigraphy and sedimentology of Holocene glacial marine deposits in the Palmer Deep, Bellingshausen Sea, Antarctica. *Mar. Geol.*

Leventer, A., Domack, E.W., Ishman, E., Brachfeld, S., McClennen, C.E., and Manley, P., 1996. Productivity cycles of 200–300 years in the Antarctic Peninsula region: understanding linkages among the sun, atmosphere, oceans, sea ice, and biota. *Geol. Soc. Am. Bull.,* 108:1626–1644.

Pittenger, A., Taylor, E., and Bryant, W.R., 1989. The influence of biogenic silica on the geotechnical stratigraphy of the Vøring Plateau, Norwegian Sea. *In* Eldholm, O., Thiede, J., Taylor, E., et al., *Proc. ODP, Sci. Results,* 104: College Station, TX (Ocean Drilling Program), 923–940.

Ronnert, L., and Mickelson, D.M., 1992. High porosity of basal till at Burroughs Glacier, southeastern Alaska. *Geology,* 20:849–852.

Figure F1. Location map of Palmer Deep, where Sites 1098 and 1099 are situated.

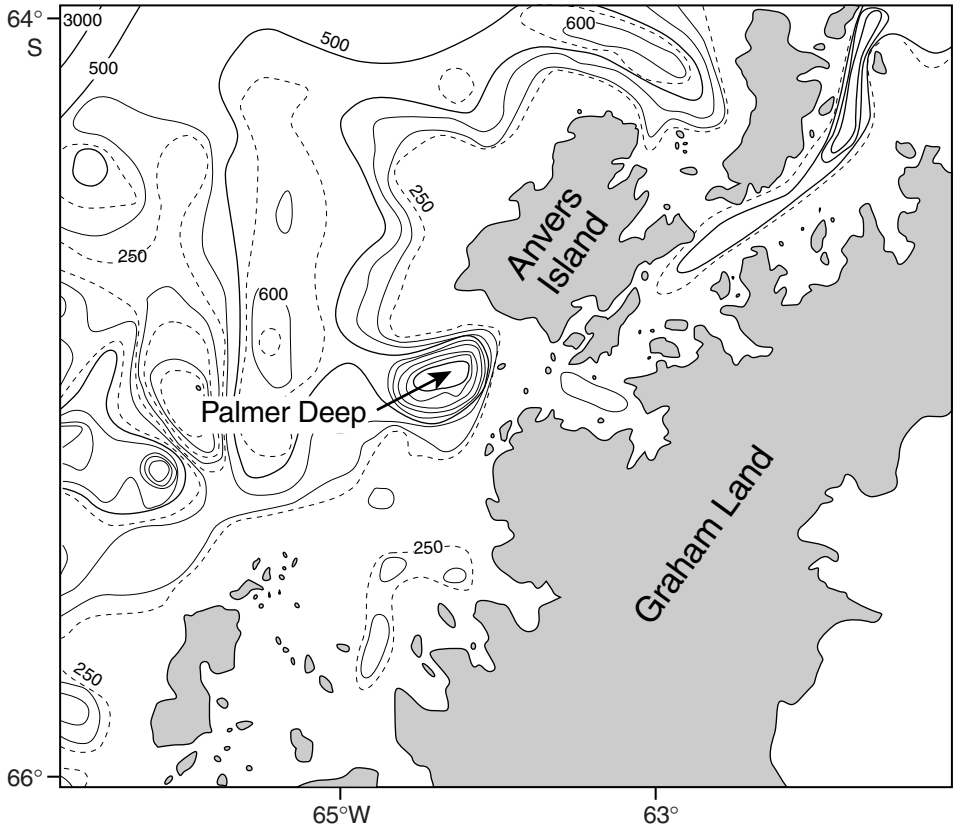

Figure F2. Locations of Sites 1098 and 1099 within Palmer Deep.

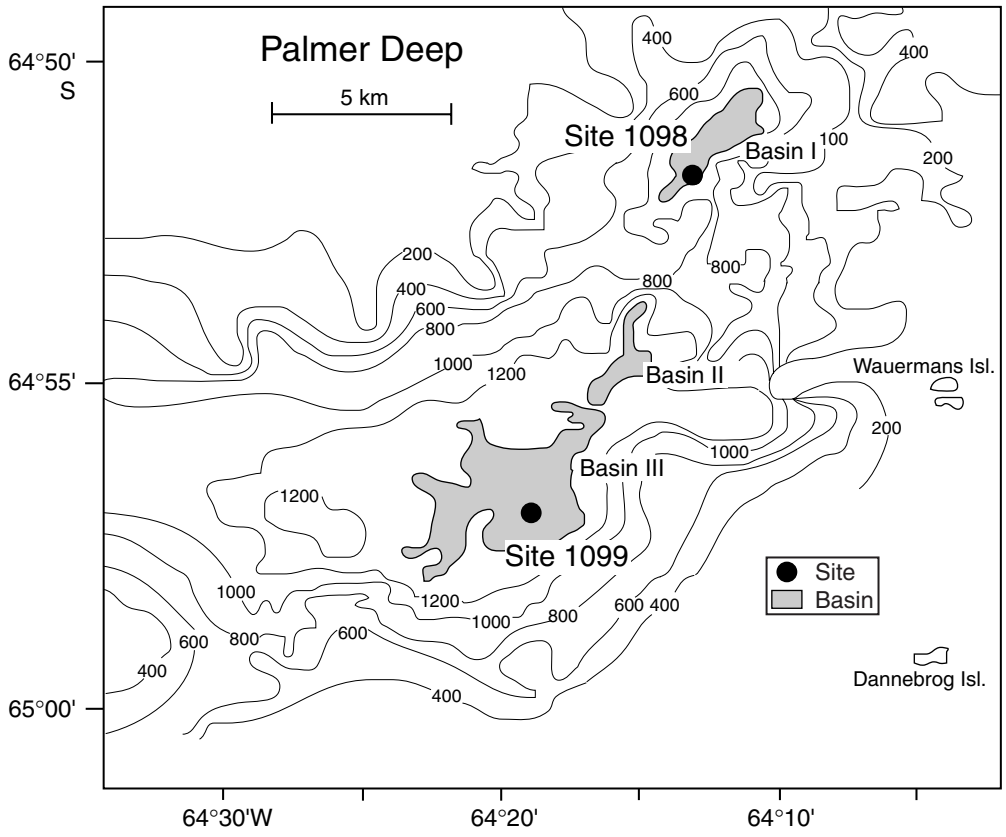

Figure F3. Lithology plotted with magnetic susceptibility and gamma ray attenuation (GRA) density for Hole 1098C.

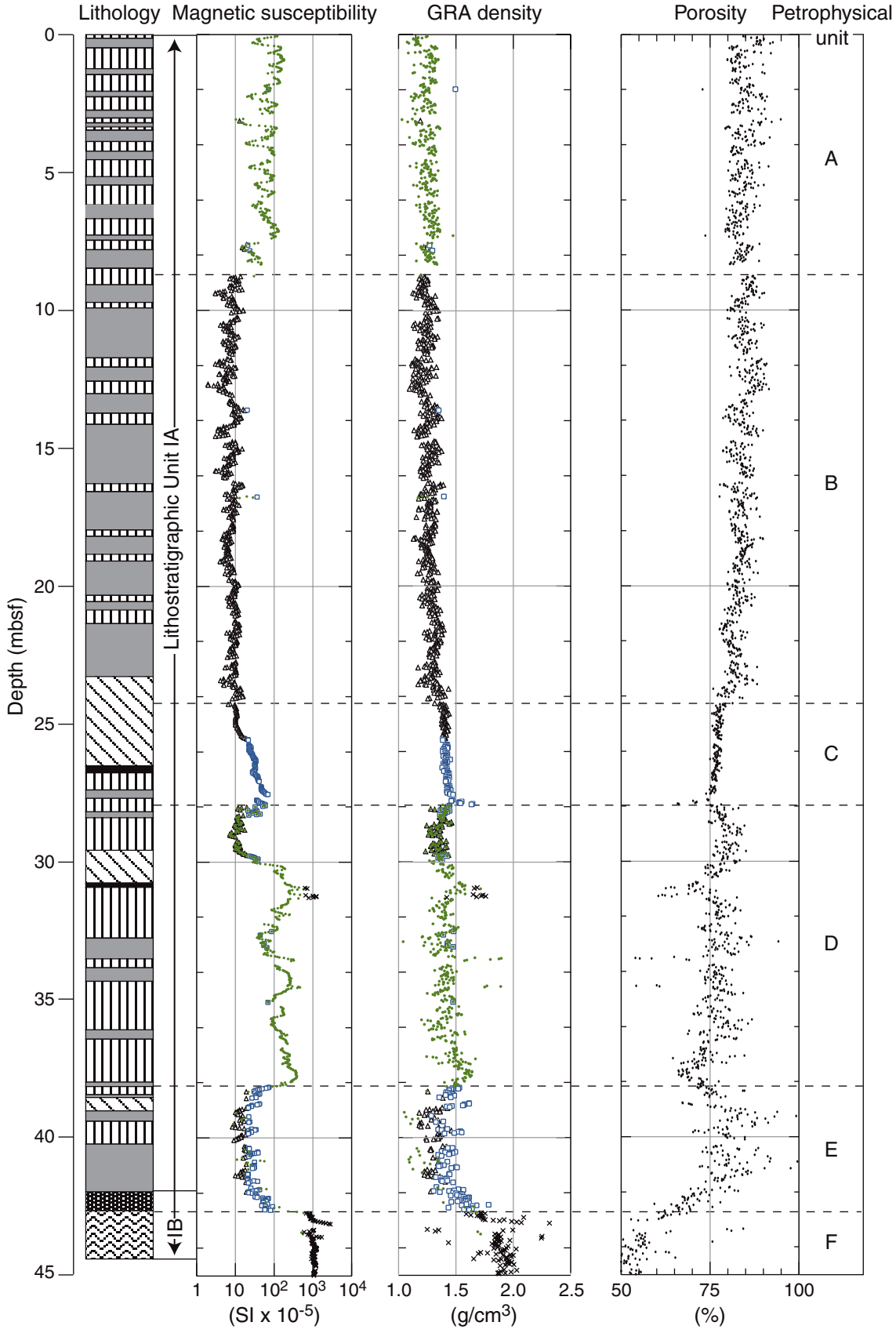

Figure F4. Lithology plotted with magnetic susceptibility and gamma ray attenuation (GRA) density for Holes 1099A and 1099B.

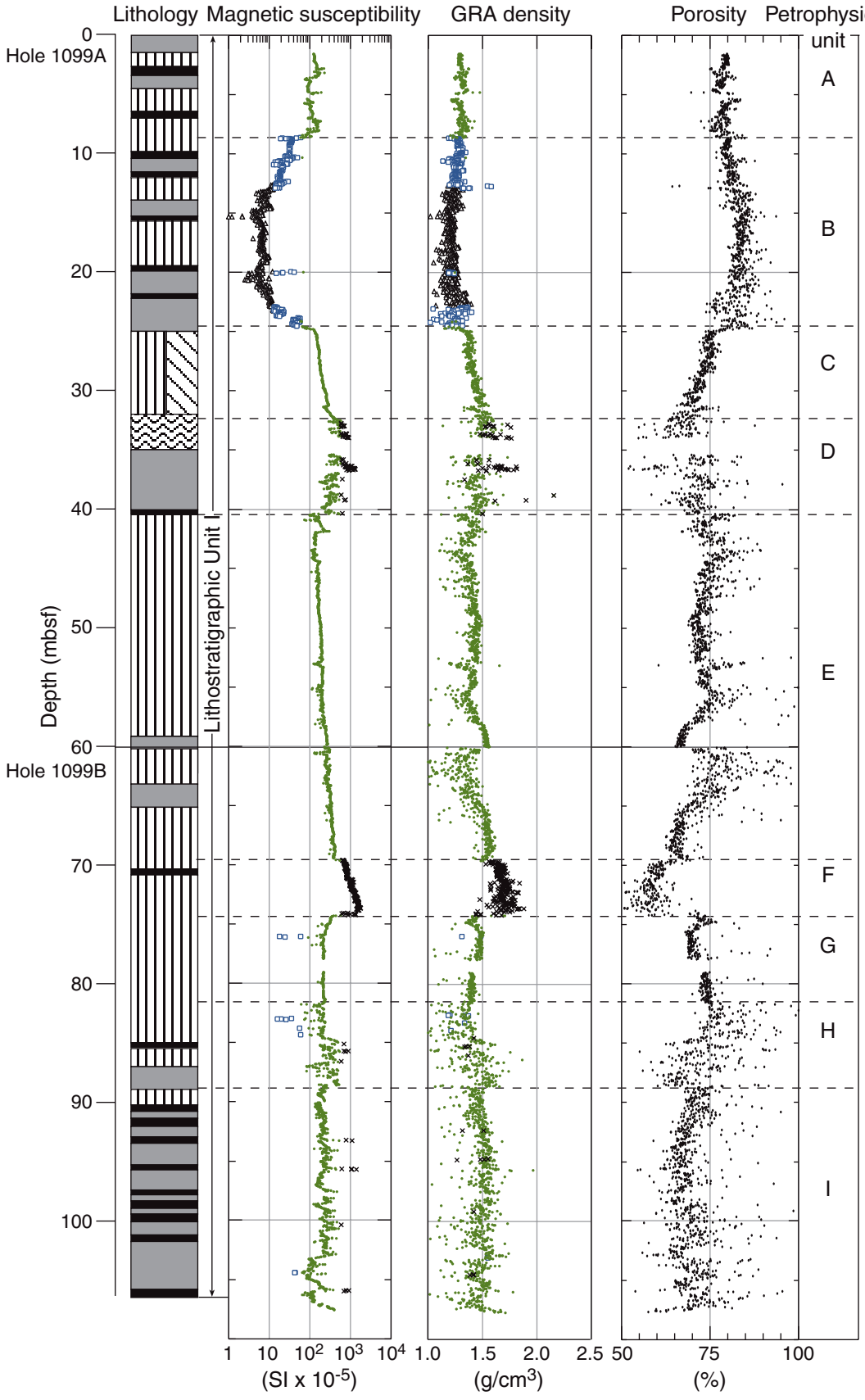

Figure F5. Lithologic and petrophysical group key for Figures F3, p. 11, and F4, p. 12.

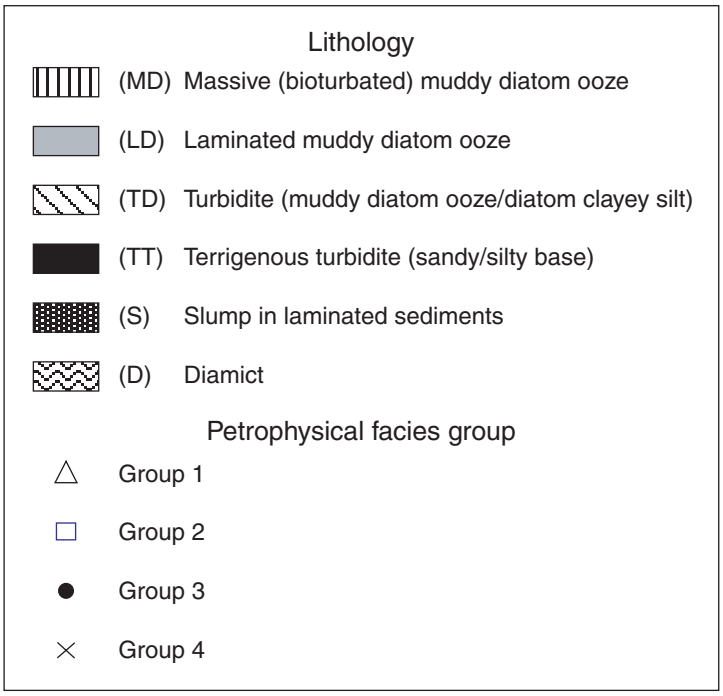

Figure F6. Discrete physical properties measurements of bulk density vs. (**A**) porosity for Holes 1098C, 1099A, and 1099B and (**B**) gamma ray attenuation (GRA) density for Hole 1098C and Site 1099.

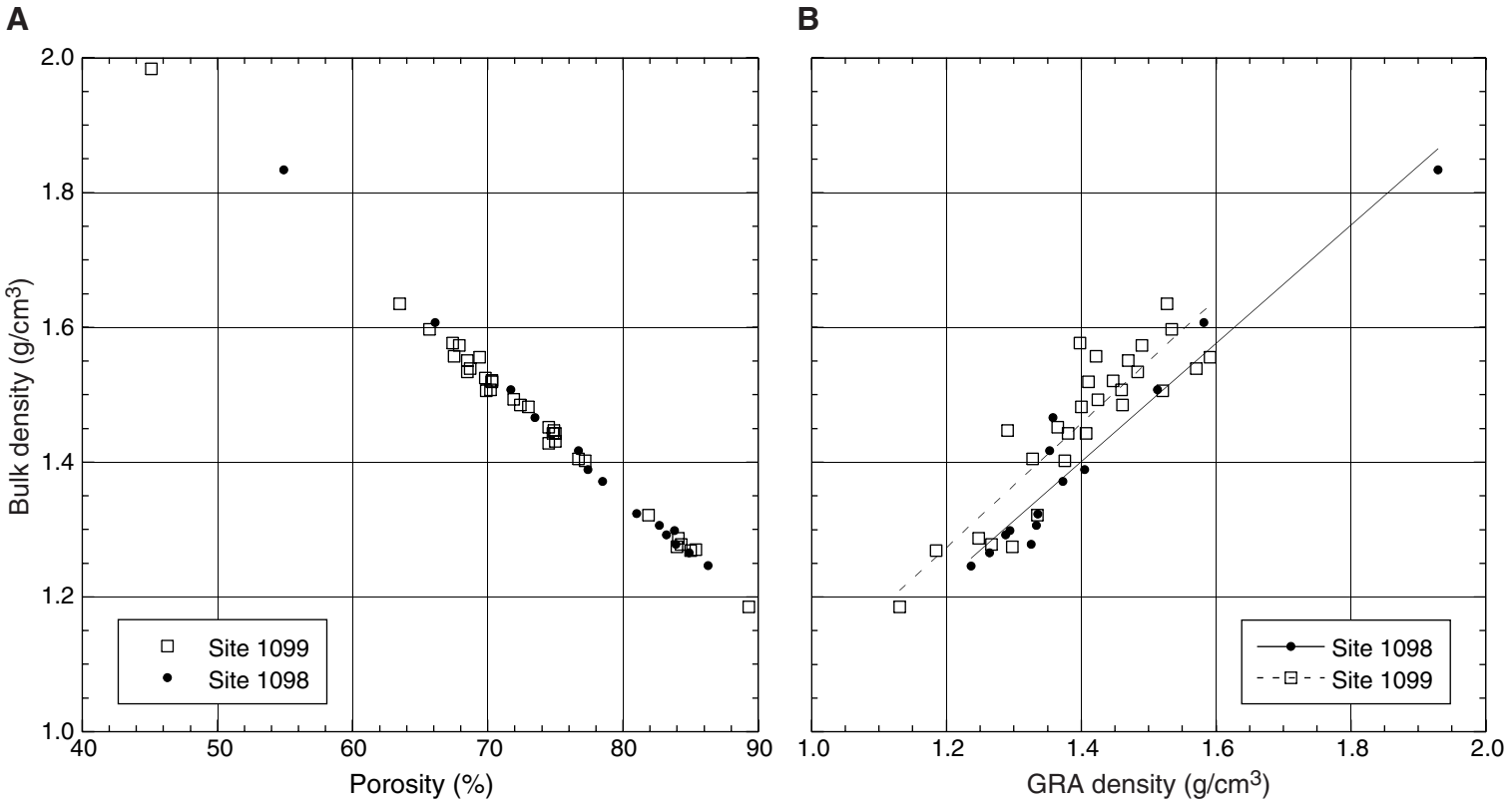

Figure F7. Gamma ray attenuation (GRA) density vs. magnetic susceptibility for (**A**) Hole 1098C and (**B**) Holes 1099A and 1099B. Data with a density <1 g/cm³ have been removed from the plots.

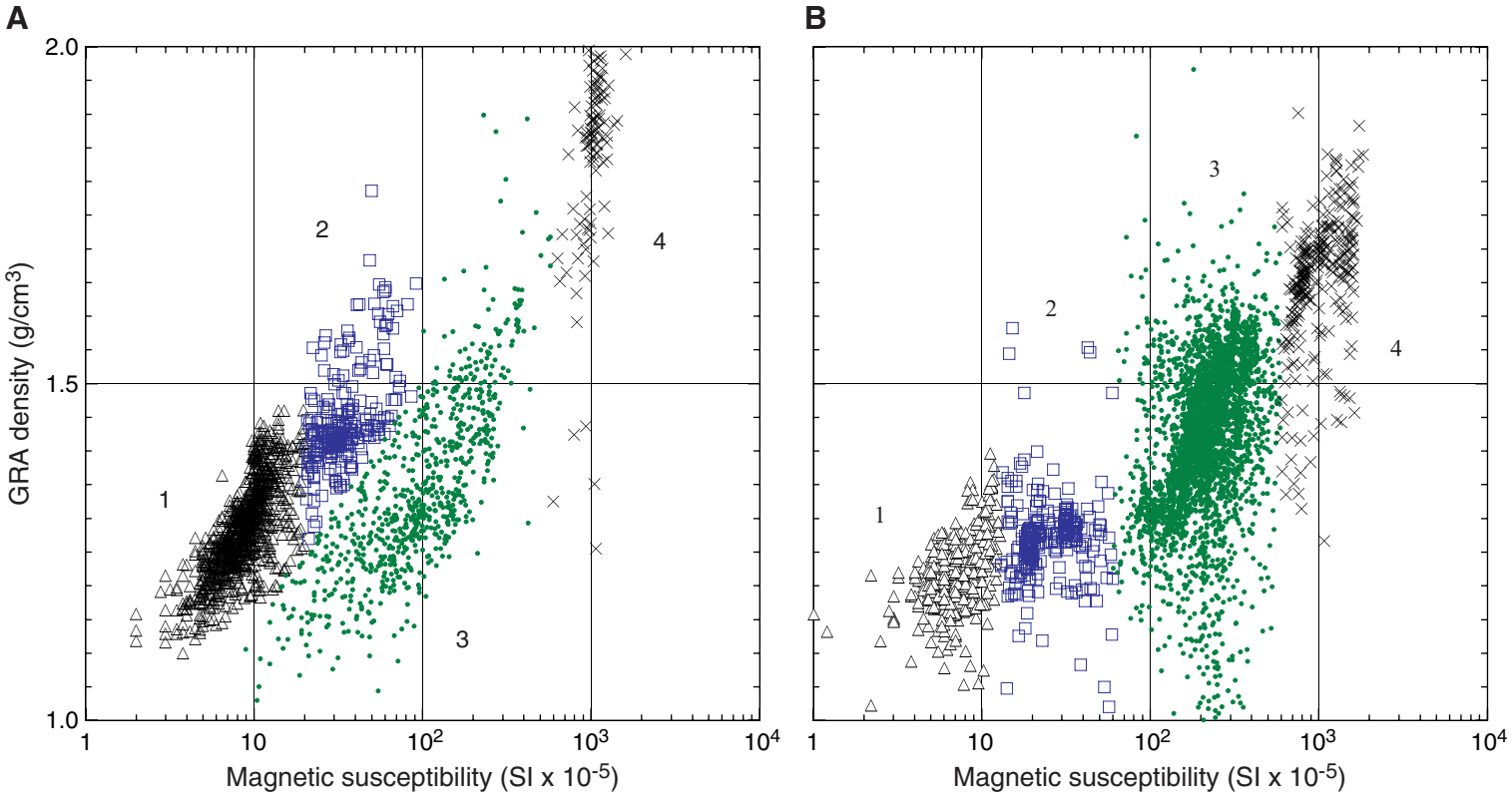

Table T1. Defining characteristics for the petrophysical units of Site 1098.

Petrophysical unit	Depth (mbsf)	Defining characteristics/lithology	Notes
A	0-~9	Muddy diatom ooze alternating every ~0.5 m between M_D and L_D. The unit consists uniquely of petrophysical Group 2.	The alternating lithologic layers can be clearly seen in the pattern of the MGS data.
B	9-24	Mostly L_D layered with M_D. There is a noticeable decrease (an order of magnitude) and smoothing of the MGS data compared with Unit A. Consists of petrophysical Group 1.	
C	24-28	Drop in variability of physical properties data compared with higher sediments. MGS and porosity data increase and decrease, respectively, with depth. The unit consists of petrophysical Groups 1 and 3 and is dominated by a turbidite between 23 and 27 mbsf, following which there is a short drop in MGS and a rise in porosity.	The depth range discrepancy between the turbidite and Unit C is clarified below.
D	28-38	Defined by its heterogeneous physical properties. The MGS varies greatly, and there is a high amount of scatter in the porosity data. There are four lithologies within this unit: M_D, L_D, T_D, and T_T. The unit consists predominantly of petrophysical Group 2, with small isolated regions of Groups 1, 3, and 4.	
E	38-43	Four lithologies: M_D, L_D, T_D, and S. There is a noticeable change in physical properties characteristics associated with this unit, mostly because the unit is banded on either side by higher MGS values. There is a gradual decrease, then increase, in the MGS and GRA data with depth in this unit; the porosity curve shows the inverse. Contains petrophysical Groups 1, 2, and 3.	It is proposed that the gradual decrease, then increase, in the MGS and GRA data with depth in this unit and the inverse porosity curve are a result of changes in grain size and sorting.
F	43-45	Corresponds with lithology D and the base of lithologic Unit IB. Defined by petrophysical Group 4.	Properties reflect poor sorting and possibly subglacial overconsolidation.

Note: M_D = massive bioturbated beds, L_D = laminated beds, T_D = muddy/clayey diatom ooze turbidite, T_T = terrigenous turbidite, S = slump laminated in sediment, D = diamict.

Table T2. Defining characteristics for the petrophysical units of Site 1099.

Petrophysical unit	Depth (mbsf)	Defining characteristics /lithology	Notes
A	1-~9	Defined by petrophysical Group 2 and the smooth character of the physical properties data. The unit is bounded by a decrease in MGS. There are three lithologies contained within this unit: M_D, L_D and T_T.	
B	9-~24	Lithologies the same as Unit A, but contains both petrophysical Groups 1 and 3. The unit has lower MGS and GRA density values compared to Unit A. There is a distinct bulge in the MGS and porosity data for this unit.	
C	24-32	Characterized by petrophysical Group 2 and the smooth physical properties data, which has a gradual incline—a signature strongly correlated with turbidites elsewhere in the two sites. Visual examination of the core produced an interpretation of mixed lithologies, M_D and T_D, in this unit.	The dual lithology interpretation present within this petrophysical unit suggests lithologic uncertainty; from the petrophysical data, it is proposed that the lithology Is more likely to be a turbidite, which could in turn affect the dating of the sequence.
D	32-41	Characterized by the change in character of the data, MGS being the most prominent. The unit consists of petrophysical Groups 2 and 4.	
E	41-69	90% lithology M_D with two layers of lithology L_D. The whole unit consists of petrophysical Group 2, reflecting the lithology of well-mixed bioturbated material. The MGS curve is notably smooth.	The joining of Holes 1099A and 1099B can be clearly seen in the GRA density and porosity data at 60 mbsf. There is likely to be a 0- to 5-m overlap, though the latter figure is large, considering the close proximity of the holes and the good recovery.
F	69-74	Consists of petrophysical Group 4 and does not correspond to the lithologic log. It shows a steady increase in MGS and GRA density and a large decrease in porosity with depth. The main lithology is M_D, with one 50-cm bed of lithology T_T.	
G	74-82	Defined by the character of the physical properties, which are all constant. The lithology is M_D and the petrophysical group is largely Group 2.	
H	82-89	Defined by highly variable physical properties data. Over the 7-m interval there are three lithologies: M_D, L_D, and T_T.	It is suggested that the properties scatter is due to the heterogeneity of the unit and the increase in pebbles observed.
I	89-108	Defined by the physical properties data, which is smooth for the MGS and GRA density data but highly scattered for the porosity data. Most of this unit consists of layers of lithology L_D and T_T, with a single 1-m layer of lithology M_D at the top of the unit. The majority of the unit consists of petrophysical Group 2, but there are isolated points of Groups 3 and 4.	

Note: M_D = massive bioturbated beds, L_D = laminated beds, T_D = muddy/clayey diatom ooze turbidite, T_T = terrigenous turbidite.